Supporting Information

The supporting information contains 10 pages and includes 12 figures and 3 tables.

High internal emission efficiency of silicon nanoparticles emitting in the visible range

Bart van Dam[a], Clara I. Osorio[b], Mark A. Hink[c], Remmert Muller[b], A. Femius Koenderink[b,a], Katerina Dohnalova[a]*

[a] Institute of Physics, University of Amsterdam, Science Park 904, 1098 XH, Amsterdam, The Netherlands.

[b] Center for Nanophotonics, AMOLF, Science Park 104, 1098 XG Amsterdam, The Netherlands.

[c] Section of Molecular Cytology and van Leeuwenhoek Centre for Advanced Microscopy, Swammerdam Institute for Life Sciences, University of Amsterdam, Science Park 904, 1098XH, Amsterdam, the Netherlands.

[*] Presently Katerina Newell

Supporting materials and methods:

Absolute external quantum efficiency (EQE): EQE was determined using the integrating sphere (IS) methodology described by *Mangolini et al.*.[1] For this we used a 10 cm IS (Newport) coupled to a spectrometer (Solar, M266) equipped with a CCD camera (Hamamatsu, S7031-1108S)

Maximum entropy method (MEM): For MEM[2] analysis, we start with 500 lifetime values equally distributed between 0 and 50 ns, with an equal starting amplitude. By optimization of the maximum likelihood estimator, the weight distribution of the lifetimes present in the studied PL decay traces was estimated. MEM eventually results even for simulated continuous lifetime distributions into multiple distinct lifetime components when performed for many iterations (>>200). To estimate the decay model that best describes our data, we therefore compare the lifetime distributions obtained using MEM analysis for our data to the distributions obtained for simulated decay traces. For this we assume different exponential decay models (stretched-exponential, bi/mono-exponential) with parameters that best fit the decay dynamics of our measured data. MEM results are shown after 200 iterations and 5000 iterations. MEM script courtesy of Dr. M. Postma (University of Amsterdam).

Structural characterization of bu:Si-NPs

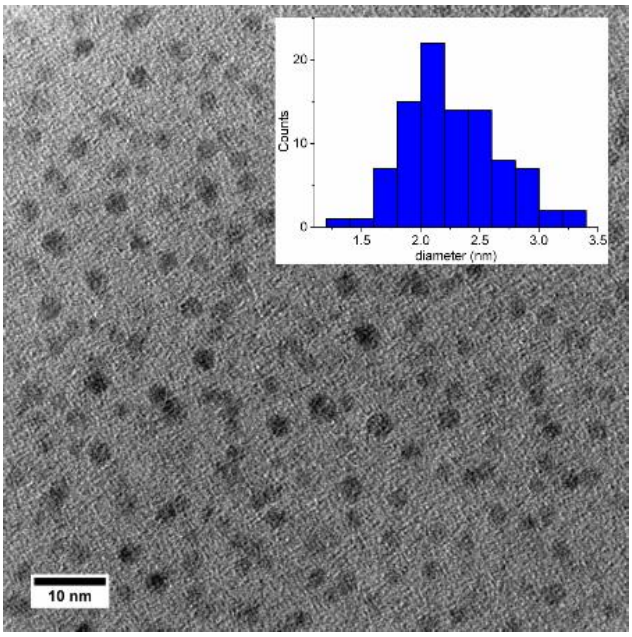

Figure S1. *Transmission electron spectroscopy (TEM) image of bu:Si-NPs with a size distribution of 2.2 ± 0.5 nm (inset).*[3]

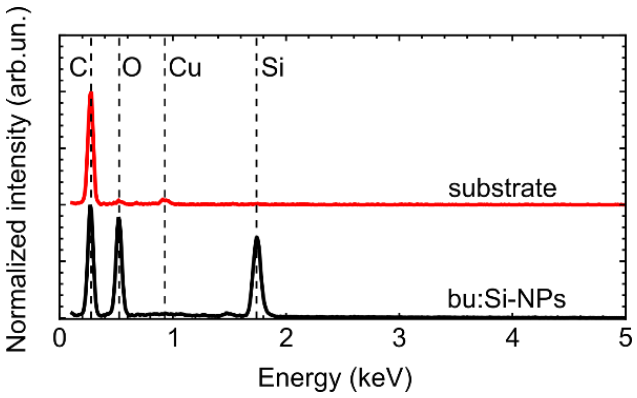

Figure S2. *Energy-dispersive X-ray (EDX) spectrum of bu:Si-NPs compared to the spectrum of only the substrate (TEM grid). The peak at around 1.74 keV shows the clear presence of silicon.*

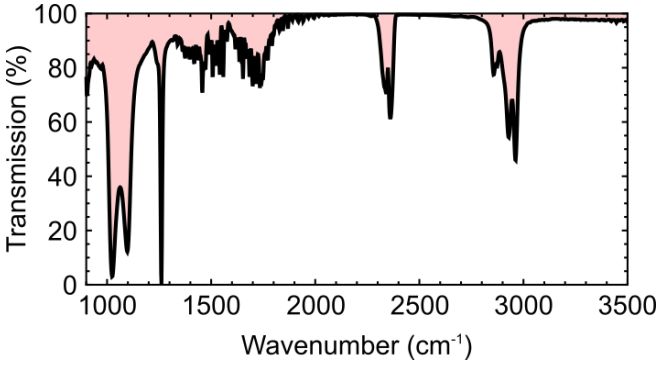

Figure S3. *Fourier-transform infrared spectrum of bu:Si-NPs.*[3]

Photoluminescence properties

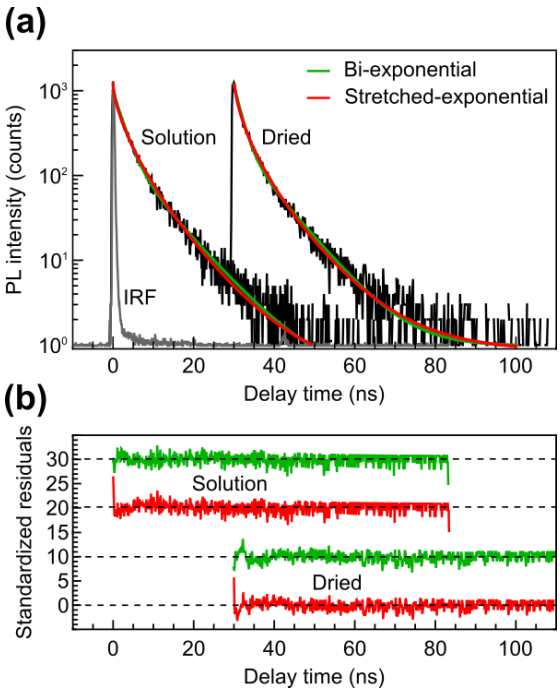

Figure S4. *(a) Time-resolved PL decay of bu:Si-NPs in ethanol and dried on a substrate. The colored lines show tail-fits of the data using a bi-exponential (green) and stretched-exponential (red) function. The bi-exponential fits yields lifetimes of 8.3 and 2.4 ns and 7.5 and 1.8 ns for bu:Si-NPs in solution and dried respectively. The stretched-exponential fits yield lifetimes of 2.1 and 1.6 ns with stretch parameters of 0.65 and 0.60. The curves are shifted along the horizontal axis for presentation purposes. (b) Weighted fit residuals. The curves are shifted along the vertical axis for presentation purposes.*

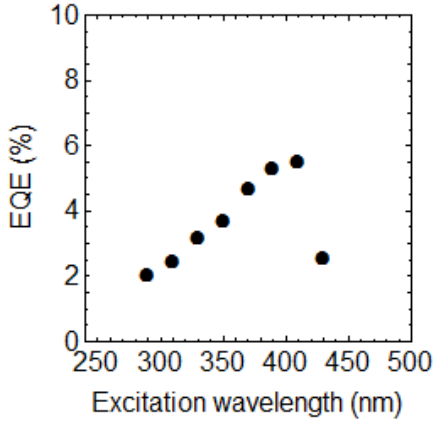

Figure S5. *Absolute external quantum efficiency of bu:Si-NPs in ethanol under different excitation wavelengths.*

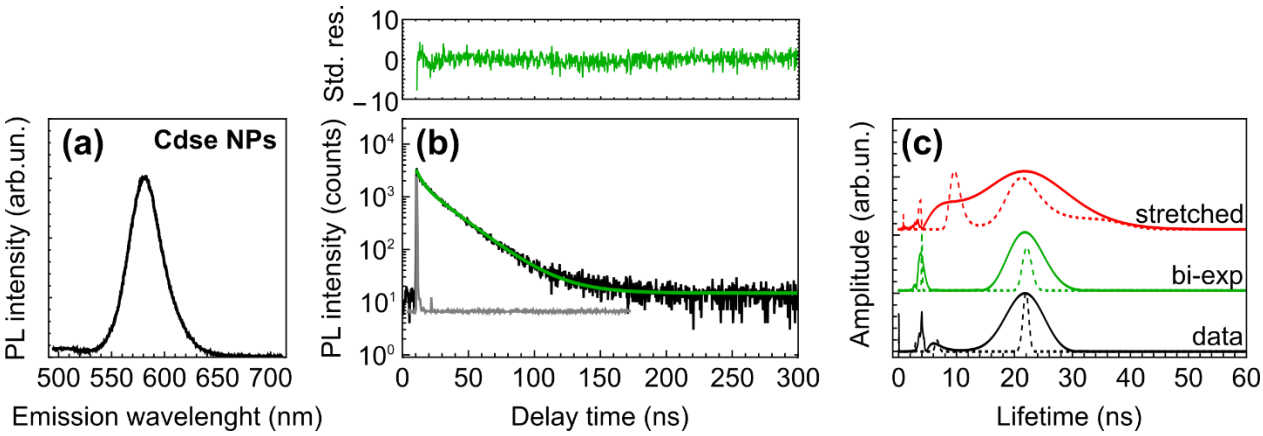

Figure S6. *(a) PL spectrum of CdSe NPs in hexane under 488 nm wavelength cw excitation. (b) PL decay under 488 nm pulsed excitation, detecting 550 ± 20 nm. The green line shows a bi-exponential fit. Standardized fitting residuals are shown in the top panel. (c) MEM[2] analysis of the PL decay of CdSe NPs in hexane (black), compared to simulated PL decays assuming a bi-exponential decay (green) and stretched-exponential decay (red). The MEM estimates the contribution of different lifetime components to a PL decay, without a priori assumptions on the distribution of lifetimes. The solid lines show the lifetime amplitudes after 200 iterations, whereas the dashed lines indicate the MEM analysis after 5000 iterations.*

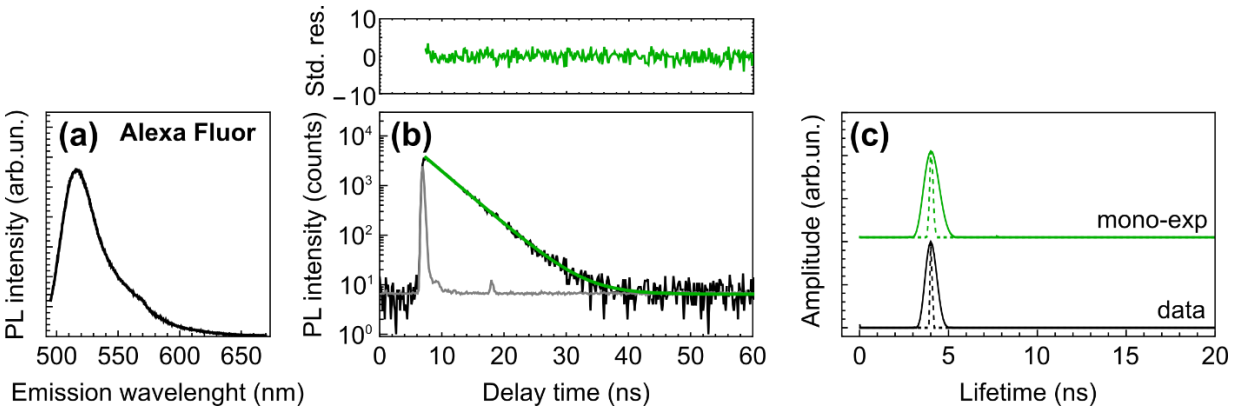

Figure S7. *(a) PL spectrum of Alexa 488 Fluor in ethanol under 488 nm wavelength cw excitation. (b) PL decay under 488 nm pulsed excitation, detecting 550 ± 20 nm. The green line shows a mono-exponential fit. Standardized fitting residuals are shown in the top panel. MEM analysis of the PL decay of Alexa Fluors in ethanol (black), compared to simulated PL decays assuming a mono-exponential decay (green). The solid lines show the lifetime amplitudes after 200 iterations, whereas the dashed lines indicate the MEM analysis after 5000 iterations.*

Local density of optical states calculations

Table S1. *Parameters used for calculations of the LDOS in Figure 2c.*

Parameter	Value
Emission wavelength	550 nm
Quartz refractive index	1.47
Emitter layer refractive index	1.47
SiO_2 refractive index	1.46
Silver refractive index	0.044 + *i* 3.6
Emitter layer thickness	15 nm
SiO_2 thickness	35 nm
Silver thickness	100 nm
Emitter position z	7.5 nm

Table S2*. Parameters used for the calculations of the LDOS in Figure 3.*

Parameter	Value			Source
	CdSe NPs	**Alexa488 Fluor**	**bu:Si-NPs**	
Emission wavelength	583 ± 10 nm	537 ± 13 nm	550 ± 20 nm	Estimated from transmission window of PL band-pass filter
Quartz refractive index	1.46	1.47	1.46	*Rodney and Spindler* [4]
Emitter layer refractive index	1.46 (1.0)	1.47 (1.0)	1.46 (1.0)	Estimated values
SiO_2 refractive index	1.46	1.46	1.46	*Malitson* [5]
Silver refractive index	(0.047 + *i* 3.9) ± *i* 0.1	(0.043 + *i* 3.5) ± *i* 0.1	(0.044+ *i* 3.6) ± *i* 0.2	*McPeak et al.*[6]
Emitter layer thickness	40 ± 10 nm	30 ± 10 nm	15 ± 5 nm	Estimated by atomic force microscopy
SiO_2 thickness	35 nm	35 nm	35 nm	EBPVD
Silver thickness	100 nm	100 nm	100 nm	EBPVD

Photoluminescence images

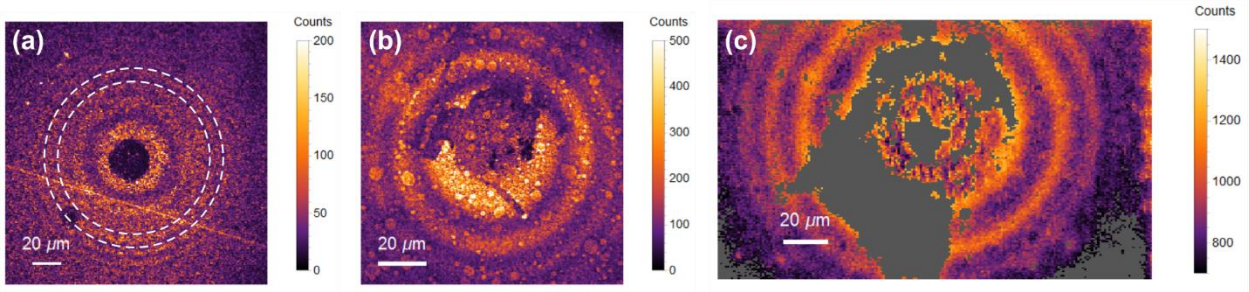

Figure S8. *Detected number of emitted photons obtained by a confocal scan of CdSe NPs (a), Alexa 488 Fluor (b) and bu:Si-NPs (c) with a spherical mirror placed on top. Examples of pixels characterized by the same substrate-mirror separation are indicated by the dashed circles. The gray areas in (c) represent parts that show increased brightness, most likely due to damage of the mirror, and have been excluded in data analysis.*

Fourier analysis

To verify that the change in decay rate with the distance to the mirror (Figure 3) is indeed due to changes in the LDOS, we perform Fourier analysis. LDOS related modulations carry a characteristic periodic signature with respect to the distance to the mirror, which directly derives from the emission wavelength. Unavoidably, the mirror also changes the excitation intensity at the emitter position as the pump beam becomes a standing wave. This means that any effect that depends on the excitation intensity, e.g. luminescence background from the mirror and non-radiative Auger recombination, will depend on the mirror-sample distance with a period that is correlated to the excitation wavelength. The Fourier analysis (Figure S9) shows that the decay rates (gray) of all samples (Figure 3) have a frequency characteristic for the emission (LDOS, red and green), and not characteristic for the excitation standing wave (blue), which confirms that the changes in the PL decay rate are due to changes in the LDOS.

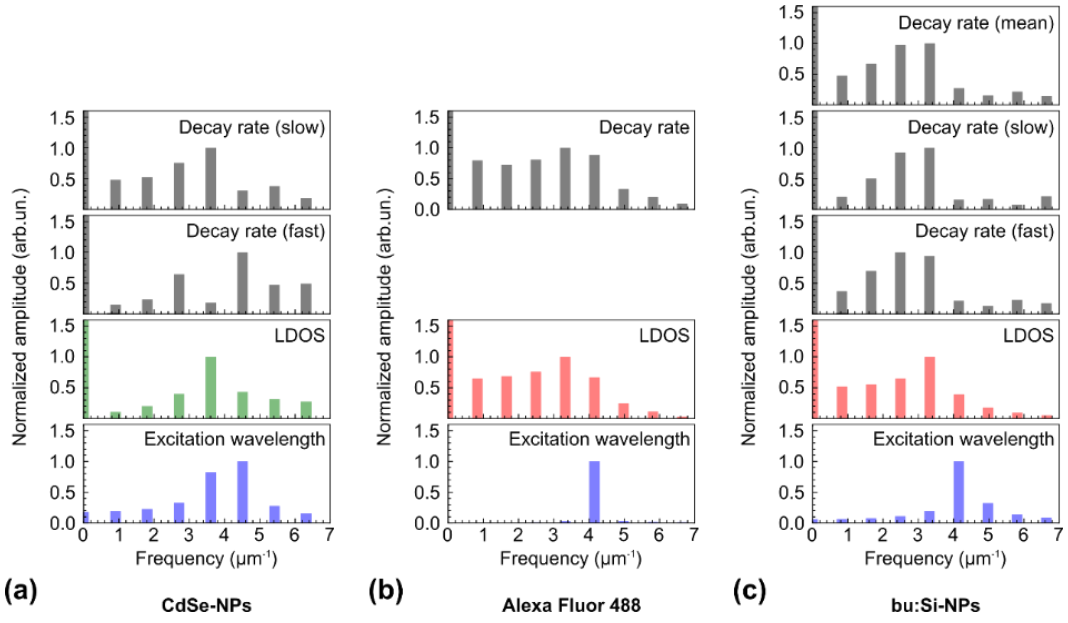

Figure S9. *Amplitudes of the fast Fourier transform of the decay rate oscillations from Figure 3 for (a) CdSe NPs, (b) Alexa Fluor 488 and (c) bu:Si-NPs. For the CdSe NPs, both the slow and fast decay components of the bi-exponential decay are shown. For the bu:Si-NPs also the mean decay rate, obtained via a stretched-exponential decay model, is shown (top panel). For comparison the amplitudes of the Fourier transform of the LDOS modulations in front of the mirror (green for isotropic LDOS, red for parallel LDOS) and of the oscillations in the pump intensity*

(blue) are also shown. The latter is simulated by a sinusoidal signal with a period equal to half of the excitation wavelength.

Substrate-mirror separation

For a spherical lens contacting the substrate, the substrate-mirror separation is given by $x = \sqrt{|\boldsymbol{r} - \boldsymbol{r_0}|^2 + R^2} - R$. However, in case the mirror sits on top of the emitter-layer or when the evaporated mirror is damaged, the actual substrate-mirror separation, d, might deviate from the calculated value: $d = x - \Delta d$. We correct for the small phase shift between the LDOS and measured decay rates by setting Δd so that the correlation between $\gamma_{PL}(d)$ and $\rho(d)$ is maximum. The calculated shifts are shown in Table S3. The 130 nm shift needed for the bu:Si-NPs measurement potentially arises from damage of the used mirror's coating. Indeed, the 130 nm is very close to the thickness of the combined silver and SiO_2 layer (135 nm, Table S2) used to create the mirror. Moreover clear irregularities are observed in the PL image for this measurement and a high intensity area is observed after removal of the mirror that is suggests a contact area layer than expected for a thin layer (<20 nm, Figure S9).

***Table S3**. Substrate-mirror separation mismatch Δd determined for all measurements.*

	CdSe NPs	**Alexa 488 Fluor**	**bu:Si-NPs**
Δd	20 nm	-50 nm	-130 nm

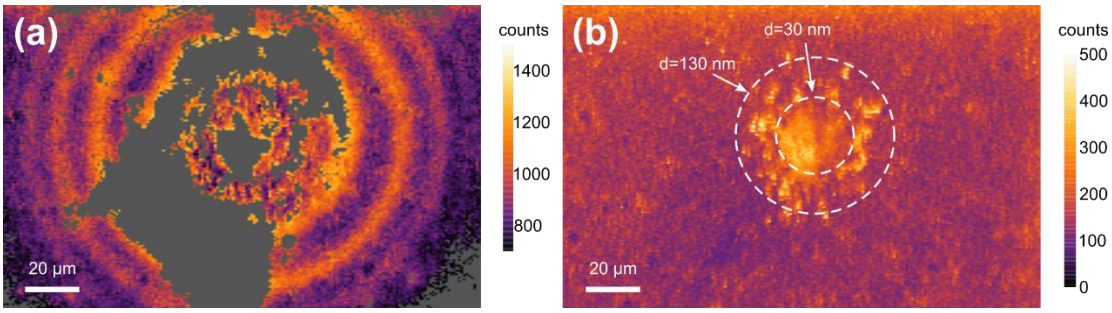

***Figure S10.** (a) Detected number of emitted photons obtained by a confocal scan of bu:Si-NPs with a spherical mirror placed on top of the sample. The gray areas represent parts that show increased brightness, most likely due to damage of the mirror, and have been excluded in data analysis. (b) Same field of view as in (a), but with the mirror removed.*

The dashed lines indicate pixels that lie within concentric rings of equal substrate-mirror separation. After removal of the mirror a bright area is observed around the contact point.

Decay dynamics of bu:Si-NPs

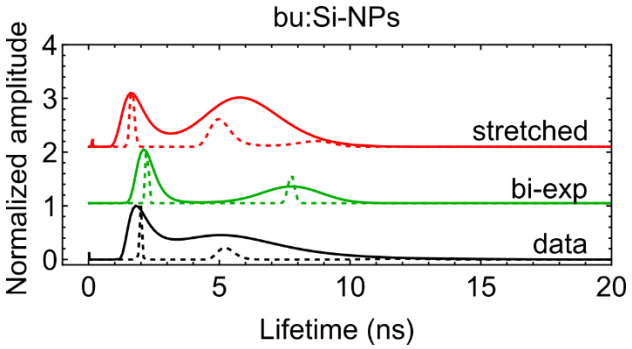

Figure S11. *MEM[2] analysis of the PL decay of bu:Si-NPs in hexane (black), compared to simulated PL decays assuming a bi-exponential decay (green) and stretched-exponential decay (red). The solid lines show the lifetime amplitudes after 200 iterations, whereas the dashed lines indicate the MEM analysis after 5000 iterations. MEM is inconclusive after 200 iterations, but shows the best agreement with the stretched-exponential model after 5000 iterations.*

Photoluminescence blinking of bu:Si-NPs

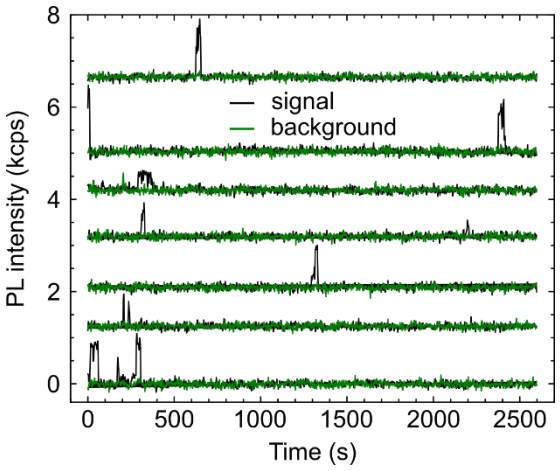

Figure S12. *PL blinking of bu:Si-NPs: Representative examples of PL intensity traces (black) under 488 nm continuous wave excitation (~30 W/cm^2) compared to the background intensity (green). Traces are shifted vertically*

for presentation purposes. The low fraction of emissive periods in each time trace shows that bu:Si-NPs are most of the time trapped in a non-emissive state.

References

(1) Mangolini, L.; Jurbergs, D.; Rogojina, E.; Kortshagen, U. Plasma Synthesis and Liquid-Phase Surface Passivation of Brightly Luminescent Si Nanocrystals. *J. Lumin.* **2006**, *121*, 327–334.

(2) Brochon, J.-C. Maximum Entropy Method of Data Analysis in Time-Resolved Spectroscopy. In *Methods in enzymology*; Academic Press, 1994; Vol. 240, pp. 262–311.

(3) Dohnalova, K.; Fucikova, A.; Umesh, C. P.; Humpolickova, J.; Paulusse, J. M. J.; Valenta, J.; Zuilhof, H.; Hof, M.; Gregorkiewicz, T. Microscopic Origin of the Fast Blue-Green Luminescence of Chemically Synthesized Non-Oxidized Silicon Quantum Dots. *Small* **2012**, *8*, 3185–3191.

(4) Rodney, W. S.; Spindler, R. J. Index of Refraction of Fused Quartz Glass for Ultraviolet, Visible, and Infrared Wavelengths. *J. Opt. Soc. Am.* **1954**, *44*, 677–679.

(5) Malitson, I. H. Interspecimen Comparison of the Refractive Index of Fused Silica. *J. Opt. Soc. Am.* **1965**, *55*, 1205–1209.

(6) Mcpeak, K. M.; Jayanti, S. V; Kress, S. J. P.; Meyer, S.; Iotti, S.; Rossinelli, A.; Norris, D. J. Plasmonic Films Can Easily Be Better: Rules and Recipes. *ACS Photonics* **2015**, *2*, 326–333.